Icarus **148**, 12–20 (2000)
doi:10.1006/icar.2000.6482, available online at http://www.idealibrary.com on IDEAL®

Fast and Slow Rotation of Asteroids

Petr Pravec

Astronomical Institute, Academy of Sciences of the Czech Republic, CZ-25165 Ondřejov, Czech Republic
E-mail: ppravec@asu.cas.cz

and

Alan W. Harris

Jet Propulsion Laboratory, 4800 Oak Grove Drive, Pasadena, California 91109

Received September 27, 1999; revised December 22, 1999

We present an analysis of the distribution of asteroid spin rates vs. size. The existence of significant populations of both slow and fast rotators among asteroids smaller than $D = 40$ km, and especially below 10 km (where our sample is mostly near-Earth asteroids), is shown. We have found that the excess of slow rotators is present at spin rates below $\approx$0.8 rev/day, and the group of fast rotators occupies the range of spin rates $>$7 rev/day. The fast rotators show interesting characteristics: The lack of objects rotating faster than 2.2 h period among asteroids with absolute magnitude $H < 22$, as well as the tendency to spheroidal shapes of fast rotators, is evidence that asteroids larger than a few hundred meters are mostly loosely bound, gravity-dominated aggregates with negligible tensile strength ("rubble piles"), while monoliths may be abundant among smaller objects. A large fraction (about half) of near-Earth fast-rotating asteroids appear to be binary systems, probably created by tidal disruptions during close encounters with the terrestrial planets.

Key Words: **asteroids, rotations; structure, rubble pile; objects, near-Earth.**

1. INTRODUCTION

Studies of asteroid rotation rates and lightcurve properties provide important data for development of theories of asteroid structure and physical processes. Although a number of significant findings were made in this field during the 20th century, we are still far from understanding the distribution of asteroid rotation rates, both overall and in detail. (For earlier reviews, see Binzel *et al.* 1989, Davis *et al.* 1989.) Especially interesting and fruitful are studies of extremes of rotation, both fast and slow rotators. During the 1990s new research projects brought a large amount of new data, extending our sample to very small asteroid sizes. Most important in this sense have been studies of lightcurve properties of near-Earth asteroids (NEAs), as they represent a sample of small (km-sized and even smaller) asteroids. In this paper, we concentrate our attention on the extremes of rotation rates, both fast and slow, which are most anomalous among the smallest asteroids.

2. SPIN DATA

We utilized lists of asteroid periods and lightcurve amplitudes compiled by A. Harris (version 1997 October) and P. Pravec (NEAs; version 1999 June). The lists are available from the authors upon request. From the lists, data for near-Earth asteroids, Mars-crossers, and main belt asteroids with quality codes $Q \geq 2$ have been selected; see Harris and Young (1983) for a description of the quality codes. (Data for Trojans and Centaurs have been excluded, but since they are large bodies this exclusion has little effect relating to our study of effects present among small asteroids.) In total, there are 750 asteroid spin periods in our sample; 631 of them are main belt asteroids (predominantly in the range $D > 10$ km), 94 are NEAs (predominantly in the range $D < 10$ km in the sample), 25 are Mars-crossers. If no diameter estimate was available, we have estimated it from the absolute magnitude, assuming a value of 0.112 for the geometric albedo p_v. This value falls reasonably in the middle of the range of measured values, and results in the absolute magnitude $H = 18$ corresponding exactly to $D = 1$ km (Tedesco *et al.* 1992). The uncertainty of such diameter estimates is likely within a factor of 1.5, and almost certainly within a factor of 2. All the data points are plotted in Fig. 1. With the exception of Section 5, we will analyze data for asteroids with $H < 22$ (D greater than about 200 m); i.e., we will exclude the two leftmost points in Fig. 1. The two smallest asteroids are excluded because they are clear outliers, both with respect to their sizes and spin rates. We will consider them separately in Section 5.

3. SLOWLY ROTATING ASTEROIDS

In the sample of 748 asteroids greater than 200 m, some objects have spin rates lower by one order of magnitude or more than most of the asteroids. They lie in the lower part of Fig. 1.

0019-1035/00 $35.00

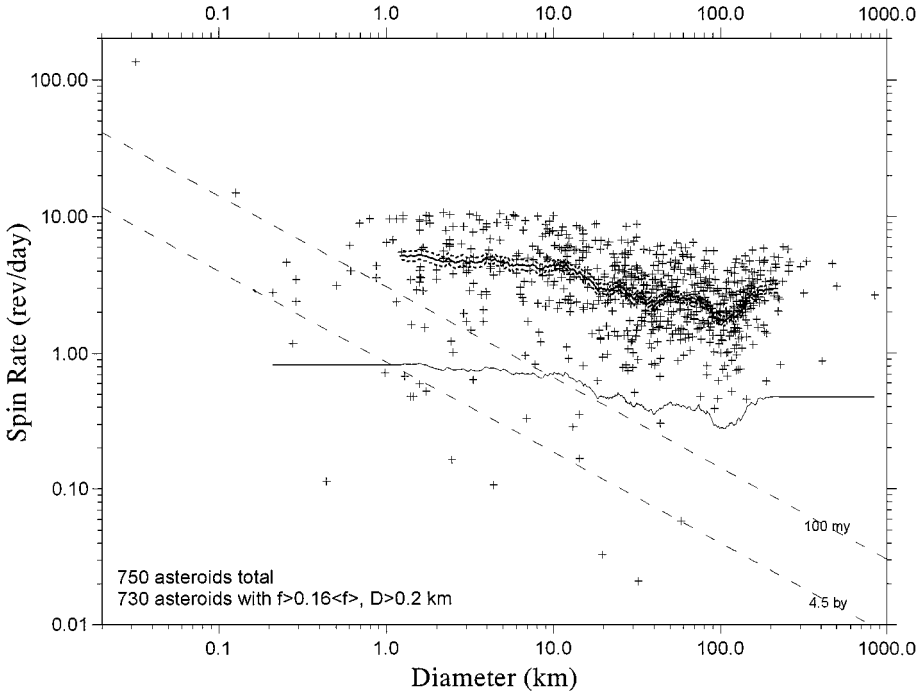

FIG. 1. Asteroids' spin rate vs diameter plot. The bold solid curve is the geometric mean spin rate $\langle f \rangle$ vs diameter, the thin solid curve is the limit $f = 0.16\langle f \rangle$ used for excluding slow rotators. Also plotted are lines of constant damping time scale τ of non-principal-axis rotational motion (thin dashed lines).

This group of slow rotators has to be characterized first, since it would affect results for the rest of the sample if left there unrecognized. Although the existence of the slow rotators population have been found by many researchers earlier (e.g., Dermott *et al.* 1984, Binzel *et al.* 1989, Fulchignoni *et al.* 1995), we are now able to better characterize this group using the present larger data set.

We have adapted a method of "running box" calculation of mean spin rate vs diameter devised by Dermott *et al.* (1984). We assumed that the distribution of spins in each subsample (within the running box) is Maxwellian with an addition of slowly rotating objects, apparent as outliers in the low spin end of the distribution. We chose to use a geometric mean spin rate $\langle f \rangle$ as it is less sensitive to outliers from the Maxwellian distributions. Nevertheless, we redid the analysis also using a mean spin rate $\bar{f}$ and found practically identical results, which indicates that our findings are not sensitive to the choice of using $\langle f \rangle$ rather than $\bar{f}$.

In computing the geometric mean spin rate of the main population, we wish to exclude the outlying slow rotators. We do this in an iterative way, first computing $\langle f \rangle$ vs diameter for all objects. We then exclude objects with spins slower than a chosen fraction c_s of $\langle f \rangle$, and then recompute $\langle f \rangle$ vs diameter. Following this iteration we recheck to see if any additional objects fall below the limit $f < c_s\langle f \rangle$, using the new values of $\langle f \rangle$. If so, we exclude them and reiterate until no further exclusions result between iterations. The value of the spin rate cut limit for slow rotators has been set conservatively to $c_s = 0.16$. The expected number of objects with $f < c_s\langle f \rangle$ from the Maxwellian distribution in a sample of 50 objects (that is the running box size we used below) is 0.16 (see Eq. (4) below); thus, an object found below the limit likely belongs to the slow rotators population. Some objects slightly above the limit $0.16\langle f \rangle$ are also possible members of the slow rotators group, but we want to be on a safe side here and therefore the conservative limit has been chosen. For this value of c_s we obtained rapid convergence, usually in only two steps. In this way we have obtained both an estimate of the population of slow rotators and the geometric mean spin rate vs diameter for the rest (actually the majority) of the objects.

The Maxwellian distribution has the form

$$n(f) = \sqrt{\frac{2}{\pi}} \frac{N f^2}{\sigma^3} \exp\left(\frac{-f^2}{2\sigma^2}\right), \tag{1}$$

where $n(f)\,\mathrm{d}f$ is the fraction of objects in the range $(f,\ f + \mathrm{d}f)$, N is the total number of objects, and σ is the dispersion. The mean spin rate and the geometric mean spin rate are related to σ,

$$\bar{f} = \sqrt{\frac{8}{\pi}}\sigma, \qquad \langle f \rangle = 1.440\sigma. \tag{2}$$

Key points of this analysis have been to choose a proper value for c_s (see above) and a suitable size of the running box. For the running box size, there is a tradeoff between the resolution in diameter (higher at smaller box sizes) and the error of the computed geometric mean spin rate within the box. After experiments with several box sizes, we fixed it at 50 objects. For this

box size, the mean error of the estimated mean spin rate for the Maxwellian distribution is 9%, and the resolution in diameter was around a few tens percent over most of the studied range of asteroid diameters in our sample (see below). We found this size to be a suitable compromise for our analysis.

In the range $D > 0.2$ km in Fig. 1, there are plotted points for 748 asteroids together with the computed $\langle f \rangle$ vs diameter and the cutoff curve for slow rotators at $0.16\langle f \rangle$. There are 18 objects with spin rates below this cutoff. We can show that this is far more than could occur by chance in the following way. From Eqs. (1) and (2), the number density (probability function) of spins for a Maxwellian distribution of N spins with geometric mean rate $\langle f \rangle$ is given by

$$n(f) \approx 2.38 \frac{N f^2}{\langle f \rangle^3} \exp\left[-1.037\left(\frac{f}{\langle f \rangle}\right)^2\right]. \quad (3)$$

For $f \ll \langle f \rangle$, the above expression can be easily integrated to obtain the number $N(<f)$ expected to have spin frequencies less than f:

$$N(<f) \approx 0.794 N \left(\frac{f}{\langle f \rangle}\right)^3. \quad (4)$$

For a total population $N = 748$, $N(<0.16\langle f \rangle) = 2.4$. We can say that the expected number of chance outliers of the main distribution that fall in our defined slow rotating population of 18 members is about 2 or 3; the rest are members of a separate population. The converse question, how many members of the "slow rotators" population actually fall above the cutoff and are hiding among the regular population is harder to answer because the population of 18 objects is not sufficient to draw statistical conclusions about the distribution of spins within this group; beyond that they are very slow. The geometric mean spin rate of this set of 18 objects is 0.055 times the geometric mean spin rate of the remaining distribution.

We can further investigate the probability that any one of the very slow rotators is a chance outlier of the main distribution of rotations. For very small values of $f/\langle f \rangle$, $N(<f)$ is less than unity and represents the probability that any one of the N objects has a spin rate less than f. The four slowest rotators of the sample, in units of $f/\langle f \rangle$, are listed in Table I. The last column of the table lists the "expected number" of members of the distribution spinning that slowly, or equivalently the probability of even one that slow. The probability of finding all four spinning so slowly is simply the product of the four individual probabilities, or $\sim 10^{-11}$. Thus it is clear that the slow-spinning population cannot possibly be just the tail end of the regular distribution.

TABLE I
Four Slowest Rotating Asteroids

Asteroid	$f/\langle f \rangle$	$N(<f)$
(288) Glauke	0.008	0.0003
(1220) Crocus	0.011	0.0008
(3691) 1982 FT	0.022	0.006
(253) Mathilde	0.023	0.007

The argument is even more general than this in that the assumption of a Maxwellian distribution is not essential to the conclusion. The constant in the equation for $N(<f)$ can be thought of as a density of spin vectors in the three-dimensional rotation frequency space near the origin of **f**. What we are observing is a clustering of vectors near the origin, and the probability we have computed is the chance that this clustering is a random fluctuation near the coordinate origin of an actually uniform distribution. Obviously it is not, so we must conclude that there is some process acting on this subset of asteroids and that is sensitive to the exact origin of the velocity space. This suggests a dissipative process that causes spin rate to decay toward zero. Chance collisions, of the type expected to produce the spins of the main sample, are not sensitive to the exact origin of the spin velocity space, which is why the expected distribution is uniform near the origin, even if not exactly Maxwellian in form at larger spin rates. Thus the conclusion to be drawn, in the most general terms, is that some subset of the asteroid sample has been altered by a dissipative process to reduce their spins toward zero. Processes that have been suggested include that (1) slow rotators are extinct comet nuclei that were slowed by outgassing processes; (2) they are binary objects which have been tidally modified, just as Earth's Moon has slowed Earth's spin rate; or (3) their spins have been modified by a radiation pressure effect, called YORP effect (Rubincam 2000). None of these processes can explain the spin of (253) Mathilde, and they do not seem very promising for other objects such as Glauke or Crocus either.

Another property of some very slowly spinning asteroids which should be mentioned is nonprincipal axis rotation, or "tumbling." Burns and Safronov (1973) calculated the timescale of damping of complex spin to principal-axis spin about the axis of maximum moment of inertia. Comparing their theoretical result to then-known spins, they concluded that all known spins should be damped to principal-axis rotation. Prompted by the discovery of the very slow spin rate of the near-Earth asteroid (4179) Toutatis and the indication that it is not in a principal-axis spin state (Ostro, pers. commun. 1993), Harris (1994) reconsidered the Burns and Safronov timescale calculation and concluded that several of the now-known asteroid spins are slow enough that damping should not have occurred in their collisional lifetime, or even in the age of the Solar System. Harris (1994) estimated the following relation between asteroid rotation period P in hours, diameter D in kilometers, and the damping time scale τ in billions of years:

$$P \approx 17 D^{2/3} \tau^{1/3}. \quad (5)$$

Lines corresponding to solutions of this relation for $\tau = 0.1$ and 4.5 billion years are plotted in Fig. 1. Clearly quite a few objects plot below these lines, indicating the possibility of

non-principal-axis spins. Toutatis has indeed been confirmed in detail to be in a non-principal-axis spin state (Hudson and Ostro 1995). To date seven asteroids have been observed with varying degrees of certainty to be likely in "tumbling" rotation states. All of these lie well below the 100-million-year damping timescale line, and all but one are below the 4.5-billion-year line. None of the other asteroids which lie below this line have been observed well enough to say for sure that their rotation is purely principal-axis; thus we conclude that tumbling rotation is the norm for slowly rotating asteroids where the damping time scale is long. This conclusion further increases the puzzle of the origin of slow rotation. If slow rotators evolve from faster rotation states through some process of dissipation, then one would expect the non-principal-axis spin to have been damped while the asteroid was spinning faster, or even as a result of the damping process itself. Yet the tumbling character persists, or perhaps increases, even while the spin rate is damped. The cause of the slow spin rates remains a complete mystery.

The population of slow rotators is significant at small sizes. The largest known slow rotator is (253) Mathilde with $D = 58$ km and $f = 0.057$ rev/day (Mottola *et al.* 1995), but the excess becomes really large below $D = 40$ km (see below). The fraction of slow rotators appears to increase with decreasing size. Considering that there is a bias against slow rotators due to the photometric techniques used for estimating the spin rates, and that this bias likely incerases with decreasing size (smaller objects are more difficult to observe long enough to detect a long period in the lightcurve), the increase of the fraction of slow rotators with decreasing size may be actually even greater than we see in the available data.

4. RAPIDLY ROTATING ASTEROIDS

The data for asteroids with $1 < D < 300$ km and $f > 0.8$ rev/day are replotted in Fig. 2, to facilitate visibility of the densest portion of Fig. 1. Arrows in the lower part of the figure indicate positions of the 25th, 75th, etc., objects of the running box analysis, so that an actual resolution and a number of independent samples in different diameter ranges can be seen. In the range of diameters greater than 40 km, we see some significant variation of the geometric mean spin rate around an average of 2.5 rev/day. These features have been discussed in Binzel *et al.* (1989). Although they would deserve a new discussion, the large asteroids can be considered as "normal" rotators; thus they are outside a scope of this paper. The limit at about 40 km marking a significant change of the spin rate distribution and being considered also as a division between "large" and "smaller" asteroids have already been found by others who generally placed it between 30 and 50 km (e.g., Binzel *et al.* 1989, Fulchignoni *et al.* 1995). As we will show below, the large asteroids group shows a distribution of the spin rates that is close to Maxwellian.

Below $D = 40$ km, there is apparent an overall increase of the geometric mean spin rate with decreasing size. The increase of the mean spin rate is steep from 40 km down to 10 km. Below 10 km, it has a significantly lower slope but still is marginally apparent. In the range 10 to 40 km, spins significantly faster than

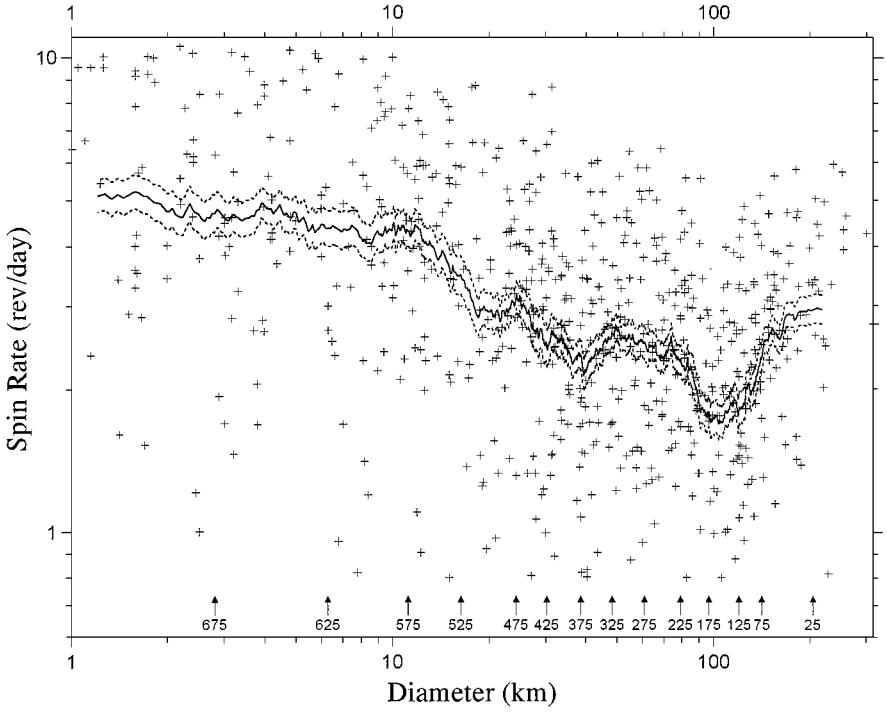

FIG. 2. The densest part of Fig. 1 shown in detail. The dashed curves represent $\pm 1\sigma$ errors of $\langle f \rangle$ (solid curve) computed from variance of a sample within the running box.

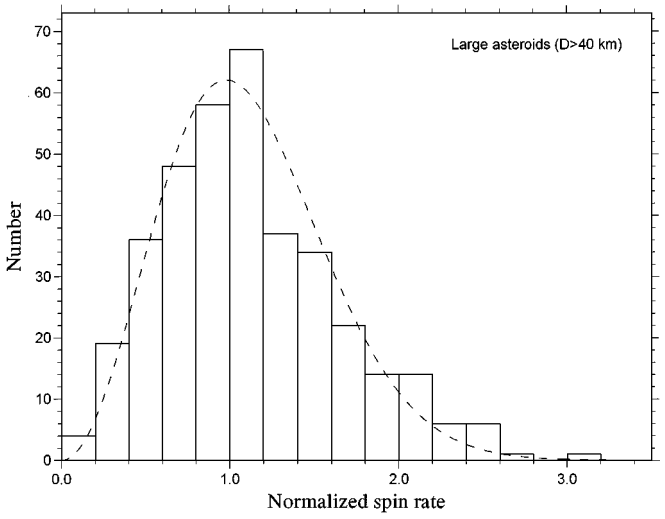

FIG. 3. Histogram of $f/\langle f \rangle$ for 367 asteroids with $D > 40$ km. The dashed curve is the corresponding Maxwellian distribution.

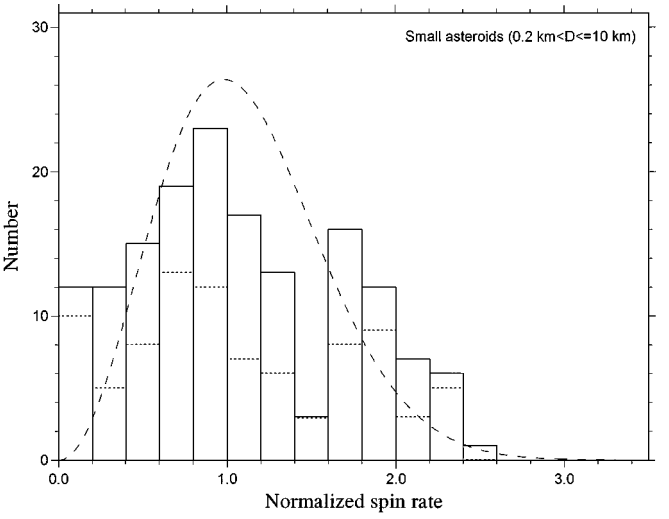

FIG. 5. Histogram of $f/\langle f \rangle$ for 156 asteroids with $D \leq 10$ km. The dashed curve is the Maxwellian distribution for the same number of objects. The short-dashed lines are the histogram for near-Earth asteroids only.

those in the large asteroids group begin to occur; while there is no large asteroid rotating faster than 7 rev/day, there is a significant (and increasing with decreasing size) fraction of such fast rotators in the 10- to 40-km range. At about 10 km, the steep increase of both the mean spin rate and the fraction of objects with $f > 7$ rev/day stops and both change only slightly below 10 km.

Using the derived geometric mean spin rate vs diameter plotted in Fig. 2, we have computed a normalized spin rate $f/\langle f \rangle$ for each asteroid. The uncertainty of the mean spin rates propagates to errors of the normalized spin rates, which are therefore about 9%. The mean spin rate dependence has been extrapolated outside the interval covered in Fig. 2 as constants equal to the last points.

In Figs. 3 to 5, we present histograms of the normalized spin rates for large, intermediate, and small asteroids. We point out that $\langle f \rangle$ used in the histograms both for binning and for drawing the Maxwellian distribution is obtained with the slow rotating population removed as described above, but in the histograms, all objects are plotted, including the slow rotators (falling into the leftmost bin in each histogram), so that their excess can be seen.

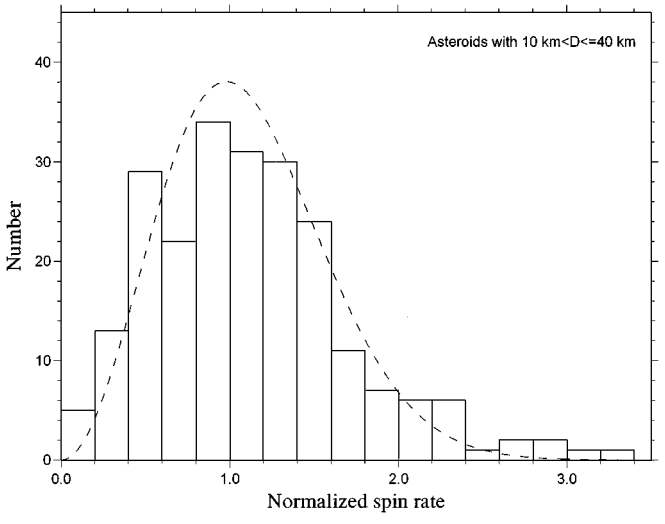

FIG. 4. Histogram of $f/\langle f \rangle$ for 225 asteroids with 10 km $< D \leq 40$ km. The dashed curve is the Maxwellian distribution for the same number of objects.

The histogram for large asteroids shows that the distribution is close to Maxwellian. In the first bin, there is an excess (though not apparent in Fig. 3 due to the coarse resolution) of one very slow rotator, (253) Mathilde; it may be considered to be an exceptional "interloper" from the smaller asteroids population rather than a regular member of the large asteroids group. The small excess at higher frequencies ($f/\langle f \rangle > 2$) is probably significant — the slightly broader distribution is consistent with the fact that the population of asteroids consists of subpopulations with different properties; specifically, the apparent excess of somewhat faster rotators can be due to faster mean spin rates of M–type asteroids and some asteroid families members (Binzel *et al.* 1989).

The histogram for mid-sized asteroids (Fig. 4) shows significant deviations from the Maxwellian distribution, at both the low- and the high-frequency ends. The histogram for small asteroids (Fig. 5) shows a remarkably non-Maxwellian distribution; there is an excess of slow rotators in the leftmost bin and a gap at $f/\langle f \rangle \approx 1.5$, apparently dividing the objects into two groups, one with a median of $f/\langle f \rangle \approx 0.8$ and the other with $f/\langle f \rangle > 1.5$. This gap is somewhat visible also in Fig. 2, as a less populated area along a curve parallel to the geometric mean spin rate curve and placed about 50% above it in the range of diameters 1 to 10 km. The detection of the gap in $f/\langle f \rangle$ is formally significant—a probability that there occurred three objects where there were expected 16 (according to the formally fitted Maxwellian distribution, see Fig. 5) is 8×10^{-5}. The Maxwellian distribution, however, does not appear relevant

there; thus we estimate the level of significance of the gap also in the following way: There are 32 objects in the three bins from $f/\langle f\rangle = 1.2$ to 1.8 in Fig. 5. If we assume a flat distribution, there are expected $\approx$11 objects in each of the three bins. The probability that there occur just three or fewer objects in the given bin is 5×10^{-3}. Thus, it appears unlikely that the gap is just a fluctuation in otherwise flat distribution but more data will be useful to increase the level of significance.

The group of asteroids above the gap has some interesting properties, and we call them "fast-rotating asteroids" (FRAs). At $D = 4$ km, the gap is placed at f about 7/d, and we take this value as an approximate limit for FRAs when using the spin rate f rather than the normalized spin rate in an analysis below.

Summarizing the above findings, we have considered three ranges of asteroid sizes with different spin characteristics. The range of large asteroids ($D > 40$ km), where the spin rate distribution is close to Maxwellian with the geometric mean spin rate varying between 1.7 and 3.0 rev/day; the range of small asteroids ($0.2 < D < 10$ km), where there is a significant excess of slow rotators (with spin rates below about 0.8/d), the geometric mean spin rate of the rest objects is 4–5 rev/day and only slightly increasing from 10 km down to 1 km, and there is the group of fast rotators; and the intermediate size range 10 to 40 km. We believe that the differences between the large and small asteroids groups are due to operations of different processes affecting their spin rates and that the intermediate size range is a transition region between these two populations.

4.1. FRA Properties: Evidence for Rubble Pile Structure

The group of fast-rotating asteroids shows interesting characteristics which give constraints to theories about their structure and physical processes. The characteristics are:

1. FRAs are missing among large ($D > 40$ km) asteroids and their population is abundant at small sizes. In the group of small asteroids ($D < 10$ km), the observed fraction of FRAs is $27 \pm 4\%$.

2. Mean lightcurve amplitude of FRAs are smaller than those of slower rotators. This is apparent from a plot of the mean observed lightcurve amplitude of near-Earth asteroids, which are most of the objects with $D < 10$ km in our sample, vs spin rate in Fig. 6. (There are also plotted points computed from all asteroids in the range $0.2 < D \leq 10$ km that are mostly within error bars of the NEA points but mostly below them, which is consistent with the fact that main belt asteroids present in the sample were observed at lower mean phase angles.) From the figure, it is also apparent that the lower mean amplitude begins to occur already for objects slightly below the approximate limit for FRAs of 7/d. The mean amplitude of NEAs with $f < 6$/d is 0.69 ± 0.05 mag, while it is 0.21 ± 0.03 mag for faster rotating NEAs. There is also apparent a continuous decrease of the mean amplitude with increasing spin rate in the range 6 to 11 rev/day. These observations indicate that FRAs are less elongated and more spheroidal than slower rotators, and the tendency to spheroidal shapes is higher for faster spin rates.

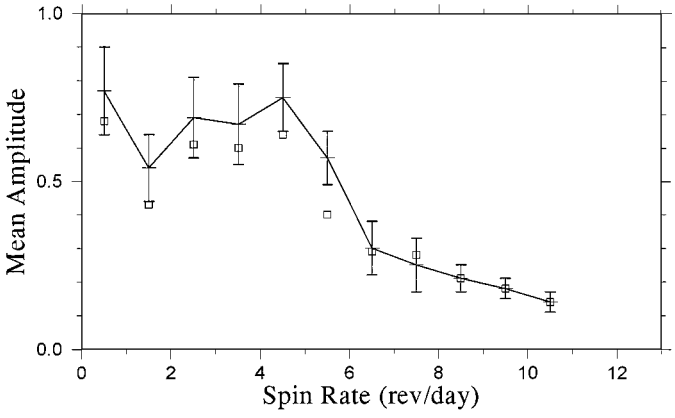

FIG. 6. The mean, observed lightcurve amplitude vs spin rate of near-Earth asteroids. The error bars are the mean errors of the means. The mean amplitudes of all asteroids with $0.2 < D \leq 10$ km are also plotted (open squares).

3. There is an apparent cutoff at the spin rate about 11 rev/day (period 2.2 h). First shown by Harris (1996), the cutoff is clearly apparent in Figs. 1 and 7, the latter showing a histogram of spin rates of near-Earth asteroids greater than about 0.2 km; both figures show that the cutoff is very abrupt.

4. FRAs are near the rotational breakup limit for aggregates with no tensile strength (so-called "rubble piles") for bulk densities plausible for asteroids (Hartmann and Larson 1967, Burns 1975, Harris 1979, 1996, and others).

The cutoff, as well as the tendency to spheroidal shapes, are evidence that FRAs larger than a few hundred meters are rubble piles. A rotating, homogeneous sphere will be everywhere in a state of compression as long as the rotation frequency does

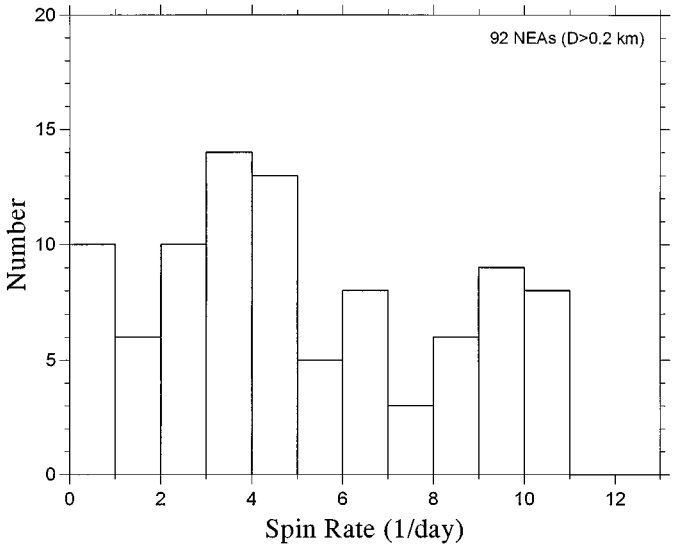

FIG. 7. Histogram of spin rates of near-Earth asteroids with $D > 0.2$ km ($H < 22$).

not exceed the surface orbit frequency about the sphere. This is simply the equivalent of saying that the centrifugal acceleration at the equator is less than the acceleration of gravity. By equating the acceleration of gravity at the surface with the centrifugal acceleration at the equator, one can derive a criterion for the critical limit of rotation period ($P_c = 2\pi/\omega_c$), depending only on the density (ρ) of the sphere,

$$\frac{Gm}{r^2} = \omega_c^2 r \Longrightarrow P_c = \frac{3.3\ \mathrm{h}}{\sqrt{\rho}}, \tag{6}$$

where G is the gravitational constant, m is the mass of the sphere, and r is its radius; ρ is expressed in g/cm^3. For a prolate spheroid, the acceleration of gravity at the tip of the long axis a is reduced from that of a sphere of the same radius a by a factor approximately equal to the axis ratio, b/a. Thus the equivalent relation for a prolate spheroid is approximately

$$P_c \approx \frac{3.3\mathrm{h}}{\sqrt{\rho}}\sqrt{\frac{a}{b}} \Longrightarrow P_c \approx 3.3\mathrm{h}\sqrt{\frac{1+\Delta m}{\rho}}, \tag{7}$$

where Δm is the full-range amplitude of lightcurve variation in magnitudes.

Figure 8 is a plot of observed NEA amplitudes vs rotation frequency with curves plotted representing the critical spin rate for bulk densities of 1.0, 2.0, and 3.0 g/cm^3. It is clear that not only is the "rotation rate barrier" for NEAs with $D > 0.2$ km consistent with an expected range of maximum bulk density of ~2–3 g/cm^3 (cf. Wilson *et al.* 1999), but the observed maximum rates of rotation appear to obey the limit of longer period for objects of greater elongation (larger lightcurve amplitude). It must be said that the above limit derivation is only approximate; in particular we take no account of triaxial rather than biaxial shapes nor of higher order variations in shape, so the results should be regarded as only approximate. Nevertheless, the sharp truncation in spin rates appears to be strong evidence that most asteroids larger than a few hundred meters in size are "strengthless" rubble piles rather than monolithic bodies. Gravity can be the only force needed to hold an asteroid body together and there is not any indication of a presence of tensile strength in asteroids greater than a few hundred meters. If there are asteroids with significant tensile strength, they must not be common, since it would be unlikely to observe the concentration of spin rates right up to the 2.2-h cutoff but none beyond it as we see in Fig. 1 at $D > 0.2$ km, if a large fraction of FRAs were monoliths.

Note: It has to be stressed that the lack of tensile strength does not mean that rubble piles are in hydrostatic equilibrium. In fact, friction and finite particle size effects prevent the bodies from forming equilibrium shapes. If rubble pile bodies formed equilibrium shapes, they would not be FRAs, since rotation periods for such objects with bulk densities plausible for asteroids have rotation period >4 h (Weidenschilling 1981).

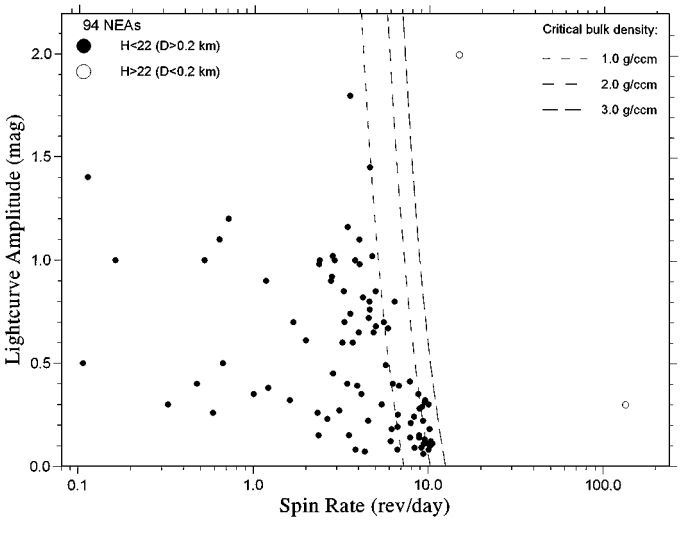

FIG. 8. The observed lightcurve amplitude vs spin rate of near-Earth asteroids.

5. SMALL MONOLITHIC ASTEROIDS

Recently, several asteroids showing periods less than 2 h have been detected. Steel *et al.* (1997) have shown that the Amor asteroid 1995 HM has a probable rotation period of 1.6 h and suggested that it is a monolith rotating under tension. The first convincing detection of a monolithic body has been done for the Apollo asteroid 1998 KY_{26}, where a period of only 10.7 min has been found (Pravec and Šarounová 1998, Ostro *et al.* 1999). 1998 KY_{26} and 1995 HM are the two leftmost points (crosses) in Fig. 1 and the two open circles in Fig. 8. They are the smallest asteroids with known spin periods; they have $H > 22$, while all other asteroids with known periods have $H < 22$ (they are larger than about 200 m). Three other small asteroids with periods from 2.5 to 20 min were found recently (Pravec *et al.* 2000a).

The theory of collisional evolution of asteroid rotation rates (Harris 1979) predicts that the mean rotation rate is constant with respect to size for gravitationally bound "strengthless" bodies, but becomes inversely proportional to D when material strength is the dominant binding force. The current statistics of rotation rates suggests that the threshold diameter is a few hundred meters (H about 22). This is in agreement with hydrodynamic computations by Love and Ahrens (1996) and Melosh and Ryan (1997) showing that asteroids as small as a few hundred meters are loosely bound, gravity-dominated aggregates, i.e., rubble piles.

6. BINARY ASTEROIDS AMONG FRAs

There are seven asteroids known to exhibit two-period lightcurves with additive components. They are interpreted as binary systems (Pravec and Hahn 1997, Pravec *et al.* 1998, Mottola *et al.* 1997, Pravec *et al.* 2000b). Estimated parameters of the seven suspected binary systems are summarized in Table II. Their short-period lightcurve components are rotation lightcurves of

TABLE II
Estimated Parameters of Binary Systems

Object	d_p (km)	d_s/d_p	a/d_p	e	P_{orb} (h)	P_{rot} (h)	A_{rot} (mag)	Taxon. class	Orb. type	Ref.[a]
1991 VH	1.2	0.40	2.7	0.07	32.69	2.6238	0.11		PHA	(1)
1994 AW_1	0.9	0.53	2.3	<0.05	22.40	2.5193	0.16		PHA	(2)
(3671)	0.9	>0.28	2.6	?	27.72	2.7053	0.16	EM	PHA	(3)
1996 FG_3	1.4	0.31	1.7	0.05	16.13	3.5942	0.09	C	PHA, VC	(4)
1999 HF_1	3.7	≥ 0.20	1.7	?	14.01	2.3191	0.14		Aten, VC	(5)
1998 PG	0.9	≥ 0.30	(1.7)	?	(14.01)	2.5162	0.13	S	Amor	(6)
(5407)	4.0	≥ 0.30	(1.7)	(<0.05)	(13.52)	2.5488	0.13	(S)	MC	(7)

Note. The diameter of the primary d_p was estimated from the effective diameter 1.0 km given by Harris and Davies (1999) for (3671), and from measured absolute magnitudes assuming the geometric albedo $p = 0.06$ for 1996 FG_3 and $p = 0.16$ for the other objects; it was corrected for $d_s/d_p = 0.4$ in cases where only a lower limit on the secondary-to-primary diameter ratio was available. a is the semimajor axis of the mutual orbit, e is its eccentricity, P_{orb} is the orbital period. P_{rot} is the rotation period of the primary, A_{rot} is its amplitude corrected for contribution of the light from the secondary. The values in parentheses are derived using the assumptions discussed in Pravec *et al.* (2000b). PHA stands for potentially hazardous asteroid, which is an object approaching to less than 0.05 AU to the Earth orbit, VC stands for Venus-crosser, MC stands for Mars-crosser. This table has been updated from Pravec *et al.* (2000b).

[a] References: (1) Pravec *et al.* (1998); (2) Pravec and Hahn (1997); (3) Mottola *et al.* (1997) + Harris and Davies (1999) + unpublished data by Pravec *et al.*; (4) Pravec *et al.* (2000b); (5) unpublished; (6) Pravec *et al.* (2000b); (7) Pravec *et al.* (2000b).

fast-spinning primaries (periods 2.3 to 3.6 h), long-period components are interpreted as mutual occultation/eclipse lightcurves in the binary systems. An independent evidence for binaries among NEAs is the presence of doublet craters on the surfaces of Earth and Venus (Bottke and Melosh 1996).

Bottke and Melosh (1996) and Richardson *et al.* (1998) proposed a theory that binaries are formed by tidal break-up of rubble pile asteroids during close encounters with the terrestrial planets. They predicted characteristics which are in qualitative agreement with the observed/estimated parameters of the seven objects (see Table II). The most important points are the following: (i) The primaries of six of the seven objects are FRAs with periods in the range 2.3 to 2.7 h; thus they are near the rotational break-up limit and the fast rotation could facilitate tidal disruption of their progenitors. (The spin rate of the seventh object, 1996 FG_3, is just below the FRAs limit of 7/day; thus it may be an outlying member of the FRAs population as well; this may be connected to its possibly lower density suggested by its C classification inferred from its color indices.) The model by Richardson *et al.* (1998) predicts mostly a moderate spin-up of primary remnants from binary NEA progenitors spinning with $P = 6$ h up to a period of 4.4 h, while the primaries of the observed binary systems actually rotate nearly twice as fast. This indicates that either the spin-up effect during the tidal splitting of NEAs is greater than predicted by the Richardson *et al.* model, or that an efficiency of the mechanism producing binary NEAs strongly depends on rotation rate of the progenitor, favoring the fastest rotators. (ii) Five of the objects approach Earth and/or Venus orbits (the two last objects from Table II are not Earth crossers at present, but their past orbital evolution might bring them to the Earth as well; Bottke, pers. commun.).

Six of the seven suspected binary system are near-Earth asteroids. (The seventh, 5407 with the perihelion distance 1.328 AU is just behind the 1.3 AU limit for Amors.) The fraction of binaries among NEAs has been estimated to be about 15% by Bottke and Melosh (1996) from the statistics of doublet craters, and by Pravec *et al.* (1999) who debiased the detection statistics of the first three known two-period NEAs and obtained an estimate that roughly 17% of NEAs (uncertainty factor 2) are binary. Since $28 \pm 6\%$ of kilometer-sized NEAs are FRAs, it appears that roughly a half of near-Earth FRAs are binary.

7. CONCLUSIONS

The existence of distinct populations of both slow and fast rotators among asteroids smaller than $D < 40$ km, and especially below 10 km, put constraints on theories of evolution of asteroids. The lack of objects rotating faster than the 2.2-h period among asteroids larger than a few hundred meters, as well as the tendency to spheroidal shapes of fast rotators is an evidence that asteroids larger than a few hundred meters are mostly loosely bound, gravity-dominated aggregates with negligible tensile strength ("rubble piles"), while monoliths may be abundant among smaller objects. A large fraction (about half) of near-Earth fast rotating asteroids are binary systems probably created by tidal disruptions during close encounters with the terrestrial planets.

ACKNOWLEDGMENTS

This work has been supported by the Grant Agency of the Academy of Sciences of the Czech Republic, Grant A3003708, and by the Grant Agency of the Czech Republic, Grant 205-99-0255. The work at JPL was supported under contract from NASA.

REFERENCES

Binzel, R. P., P. Farinella, V. Zappalà, and A. Cellino 1989. Asteroid rotation rates: Distributions and statistics. In *Asteroids II* (R. P. Binzel, T. Gehrels, and M. S. Matthews, Eds.), pp. 416–441. Univ. of Arizona Press, Tucson.

Bottke, W. F., and H. J. Melosh 1996. Binary asteroids and the formation of doublet craters. *Icarus* **124**, 372–391.

Burns, J. A. 1975. The angular momenta of Solar System bodies: Implications for asteroid strengths. *Icarus* **25**, 545–554.

Burns, J. A., and V. S. Safronov 1973. Asteroid nutation angles. *Mon. Not. R. Astron. Soc.* **165**, 403–411.

Davis, D. R., S. J. Weidenschilling, P. Farinella, P. Paolicchi, and R. P. Binzel 1989. Asteroid collisional history: Effects on sizes and spins. In *Asteroids II* (R. P. Binzel, T. Gehrels, and M. S. Matthews, Eds.), pp. 805–825. Univ. of Arizona Press, Tucson.

Dermott, S. F., A. W. Harris, and C. D. Murray 1984. Asteroid rotation rates. *Icarus* **57**, 14–34.

Fulchignoni, M., M. A. Barucci, M. Di Martino, and E. Dotto 1995. On the evolution of the asteroid spin. *Astron. Astrophys.* **299**, 929–932.

Harris, A. W. 1979. Asteroid rotation rates. II. A theory for the collisional evolution of rotation rates. *Icarus* **40**, 145–153.

Harris, A. W. 1994. Tumbling asteroids. *Icarus* **107**, 209–211.

Harris, A. W. 1996. The rotation rates of very small asteroids: Evidence for "rubble pile" structure. *Proc. Lunar Planet. Sci. Conf. 27th*, 493–494.

Harris, A. W., and J. K. Davies 1999. Physical characteristics of near-Earth asteroids from thermal infrared spectrophotometry. *Icarus* **142**, 464–475.

Harris, A. W., and J. W. Young 1983. Asteroid rotation. IV. 1979 Observations. *Icarus* **54**, 59–109.

Hartmann, W. K., and S. M. Larson 1967. Angular momenta of planetary bodies. *Icarus* **7**, 257–260.

Hudson, R. S., and S. J. Ostro 1995. Shape and non-principal axis spin state of asteroid 4179 Toutatis. *Science* **270**, 84–86.

Love, S. G., and T. J. Ahrens 1996. Catastrophic impacts on gravity dominated asteroids. *Icarus* **124**, 141–155.

Melosh, H. J., and E. V. Ryan 1997. Asteroids: Shattered but not dispersed. *Icarus* **129**, 562–564.

Mottola, S., G. Hahn, P. Pravec, and L. Šarounová 1997. S/1997 (3671) 1. *IAU Circ.* 6680.

Mottola, S., W. D. Sears, A. Erikson, A. W. Harris, J. W. Young, G. Hahn, M. Dahlgren, B. E. A. Mueller, B. Owen, R. Gil-Hutton, J. Licandro, M. A. Barucci, C. Angeli, G. Neukum, C.-I. Lagerkvist, and J. F. Lahulla 1995. The slow rotation of 253 Mathilde. *Planet. Space Sci.* **43**, 1609–1613.

Ostro, S. J., P. Pravec, L. A. M. Benner, R. S. Hudson, L. Šarounová, M. D. Hicks, D. L. Rabinowitz, J. V. Scotti, D. J. Tholen, M. Wolf, R. F. Jurgens, M. L. Thomas, J. D. Giorgini, P. W. Chodas, D. K. Yeomans, R. Rose, R. Frye, K. D. Rosema, R. Winkler, and M. A. Slade 1999. Radar and optical observations of asteroid 1998 KY_{26}. *Science* **285**, 557–559.

Pravec, P., and G. Hahn 1997. Two-period lightcurve of 1994 AW_1: Indication of a binary asteroid? *Icarus* **127**, 431–440.

Pravec, P., and L. Šarounová 1998. 1998 KY_{26}. *IAU Circ.* 6941.

Pravec, P., M. Wolf, and L. Šarounová 1998. Occultation/eclipse events in binary asteroid 1991 VH. *Icarus* **133**, 79–88.

Pravec, P., M. Wolf, and L. Šarounová 1999. How many binaries are there among near-Earth asteroids? In *Proc. IAU Coll. 173* (J. Svoreň, E. M. Pittich, and H. Rickman, Eds.), pp. 159–162. Astron. Inst. Slovak Acad. Sci., Tatranská Lomnica.

Pravec, P., C. Hergenrother, R. Whiteley, L. Šarounová, P. Kušnirák, and M. Wolf 2000a. Fast rotating asteroids 1999 TY_2, 1999 SF_{10}, and 1998 WB_2. *Icarus* **147**, 477–486.

Pravec, P., L. Šarounová, D. L. Rabinowitz, M. D. Hicks, M. Wolf, Yu. N. Krugly, F. P. Velichko, V. G. Shevchenko, V. G. Chiorny, N. M. Gaftonyuk, and G. Genevier 2000b. Two-period lightcurves of 1996 FG_3, 1998 PG, and (5407) 1992 AX: One probable and two possible binary asteroids. *Icarus* **146**, 190–203.

Richardson, D. C., W. F. Bottke, and S. G. Love 1998. Tidal distortion and disruption of Earth-crossing asteroids. *Icarus* **134**, 47–76.

Rubincam, D. P. 2000. Radiative spin-up and spin-down of small asteroids. *Icarus*, in press.

Steel, D. I., R. H. McNaught, G. J. Garradd, D. J. Asher, and A. D. Taylor 1997. Near-Earth asteroid 1995 HM: A highly-elongated monolith rotating under tension? *Planet. Space Sci.* **45**, 1091–1098.

Tedesco, E. F., G. J. Veeder, J. W. Fowler, and J. R. Chillemi 1992. *The IRAS Minor Planet Survey.* Tech. Rep. PL-TR-92-2049. Phillips Laboratory, Hanscom AF Base, MA.

Weidenschilling, S. J. 1981. How fast can an asteroid spin? *Icarus* **46**, 124–126.

Wilson, L., K. Keil, and S. J. Love 1999. The internal structures and densities of asteroids. *Meteoritic Planet. Sci.* **34**, 479–483.